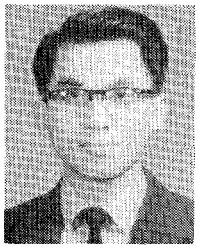

Fung I. Tseng (M'66) was born in Pingtung, Taiwan, on January 12, 1936. He received the B.S.E.E. degree from Taiwan University, Taipei, Taiwan, in 1958, the M.S. degree from Chiao-Tung University, Hsin-Chu, Taiwan, in 1961, and the Ph.D. degree from Syracuse University, Syracuse, NY, in 1966.

From 1966 to 1969 he was a Research Engineer at Syracuse University. Since 1969 he has been on the faculty of the Rochester Institute of Technology, Rochester, NY, where he has been engaged in teaching and research on electromagnetic waves and antenna arrays.

Dr. Tseng is a member of Phi Tau Phi Scholastic Honor Society and Commission B of URSI.

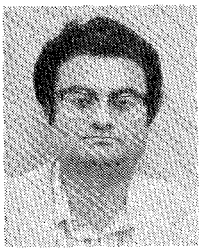

Tapan K. Sarkar (S'69-M'76) was born in Calcutta, India on August 2, 1948. He received the B.Tech. degree from the Indian Institute of Technology, Kharagpur, India, in 1969, the M.Sc.E. degree from the University of New Brunswick, Fredericton, Canada, in 1971, and the M.S. and Ph.D. degrees from Syracuse University, Syracuse, NY, in 1975.

From 1969 to 1971, he served as an Instructor at the University of New Brunswick. While studying at Syracuse University, he served as an Instructor and Research Assistant in the Department of Electrical and Computer Engineering, where he is presently an Adjunct Assistant Professor. Since 1976 he has been an Assistant Professor at the Rochester Institute of Technology, Rochester, NY. From 1977 to 1978 he was a Research Fellow at the Gordon McKay Laboratory of Harvard University, Cambridge, MA. His current research interests deal with system identification, signal processing, and analysis of electrically large electromagnetic systems.

Dr. Sarkar is a member of Sigma Xi and URSI Commission B.

Donald D. Weiner (S'54-M'60) was born in Boston, MA on October 30, 1934. He received the S.B. and S.M. degrees from M.I.T., Cambridge, MA, in 1956 and 1958, and the Ph.D. degree from Purdue University, W. Lafayette, IN, in 1964, all in electrical engineering.

He has worked for Philco Corporation, General Electronic Laboratories, and the Sylvania Applied Research Laboratory, and has taught at M.I.T., the University of Miami, Coral Gables, FL, Purdue University, and Syracuse University, Syracuse, NY. He joined Syracuse University in 1964 as an Assistant Professor in the Department of Electrical and Computer Engineering where he became a Full Professor in 1973. He is a coauthor (with John Spina) of *Sinusoidal Analysis and Modeling of Weakly Nonlinear Circuits* (Princeton, NJ: Van Nostrand Reinhold, 1980). His current research deals with interference effects in digital circuits.

Kalman Filtering in Two Dimensions: Further Results

JOHN W. WOODS, MEMBER, IEEE, AND VINAY K. INGLE, MEMBER, IEEE

Abstract—**The two-dimensional reduced update Kalman filter was recently introduced. The corresponding scalar filtering equations were derived for the case of estimating a Gaussian signal in white Gaussian noise and were shown to constitute a general nonsymmetric half-plane recursive filter. This paper extends the method to the deconvolution problem of image restoration. This paper also provides a more thorough treatment of the uniquely two-dimensional boundary condition problems. Numerical and subjective examples are presented.**

I. Introduction

KALMAN filtering methods have been very useful in one-dimensional (1-D) digital signal processing. In [1] the Kalman filtering method was generalized to two dimensions in a computationally efficient manner. For the case of scalar observations, computational efficiency was obtained through the use of a reduced update procedure. Scalar filtering equations were obtained for the undistorted signal-in-noise observation model. The signal model was of the AR type with a general or nonsymmetric half-plane (NSHP) coefficient support. The resulting filter equations were seen to constitute an NSHP recursive filter. Furthermore, the approach resulted in a very efficient steady-state filter for application to homogeneous images or other 2-D data. The filter was shown to be weakly optimal [2] and also approximately strongly optimal in several examples.

In many applications of two-dimensional (2-D) filtering, one observes a noisy and distorted version of the signal and wishes to estimate the noise-free signal. This is the case, for example, in image restoration [3]. Thus, it is of interest to extend the reduced update Kalman filter (RUKF) to these deconvolution type problems. This is accomplished in the present paper through modeling signal distortion as an FIR filtering with NSHP support.

In Kalman filtering, it is necessary to have appropriate initial conditions so that the overall estimate will be optimal. This

Manuscript received November 16, 1978; revised January 23, 1980. This research was supported by the U.S. Air Force Office of Scientific Research, Air Force Systems Command, under Grant 77-3361.

The authors are with the Department of Electrical and Systems Engineering, Rensselaer Polytechnic Institute, Troy, NY 12181.

0096-3518/81/0400-0188$00.75

can be especially important for the first few data points. Likewise in 2-D Kalman filtering, it is necessary to properly consider the possibly random boundary conditions. This will be accomplished by augmenting the global state vector [1] to allow random boundary conditions.

We start with a brief review of the RUKF. This is followed by the extension to include the possibility of signal distortion as mentioned above. Next, a detailed discussion of the uniquely two-dimensional boundary value problems is presented. Finally, examples are shown based on simulations using both real and synthetic image data.

II. Review of RUKF

This section will review some of the important features of the RUKF derived in [1]. The notation is that used in [1] and [4].

The signal model is Markov and is given as an NSHP recursive model

$$s(m,n) = \sum_{\mathcal{R}_{\oplus+}} c_{kl}\, s(m-k, n-l) + w(m,n) \tag{1}$$

where $w(m,n)$ is a white Gaussian noise field. Also, $\mathcal{R}_{\oplus+} = \{k \geq 0, l \geq 0\} \cup \{k < 0, l > 0\}$ and $c_{00} = 0$. The model (1) can be thought of as a 2-D recursive filtering of the input field w. We assume this filter is $(M \times M)$th order [4].

The observation equation is given as

$$r(m,n) = s(m,n) + v(m,n) \tag{2}$$

where v is a white Gaussian source. The model and observation equations in vector form are

$$\boldsymbol{s}(m,n) = \boldsymbol{C}\boldsymbol{s}(m-1,n) + \boldsymbol{w}(m,n) \tag{3}$$

$$r(m,n) = \boldsymbol{h}^T \boldsymbol{s}(m,n) + v(m,n) \tag{4}$$

with $\boldsymbol{h}^T = (1, 0, \cdots, 0)$. We solve these equations in a square region $I \triangleq [1, N]^2$ with known deterministic boundary values on the top and sides. For convenience these boundary values are taken to be zero. If the known boundary values were nonzero, the filtering equations could be straightforwardly modified to account for this deterministic input. (The case of random boundary values is discussed in Section III.) Then through conventional line-by-line scanning we convert this 2-D problem into an equivalent 1-D problem with global state vector

$$\begin{aligned}\boldsymbol{s}(m,n) \triangleq [&s(m,n), s(m-1,n), \cdots, s(1,n);\\ &s(N,n-1), \cdots, s(1,n-1); \cdots;\\ &s(N,n-M), \cdots, s(m-M+1,n-M)]^T.\end{aligned} \tag{5}$$

This scanning or total ordering of the spatial points, thus establishes a past–present–future relation on the data. Thus, we can speak of causal filtering referring to this ordering. The Kalman filtering equations with the above interpretation of the $\boldsymbol{s}$ vector can immediately be written down. The difficulty with these equations is the amount of computation and memory requirements associated with them. By limiting the update procedure to only those elements "near" the "present" point, the wasteful computations can be avoided, thereby increasing the efficiency of the algorithm. A reduced update constraint is then applied to update only the local state vector.

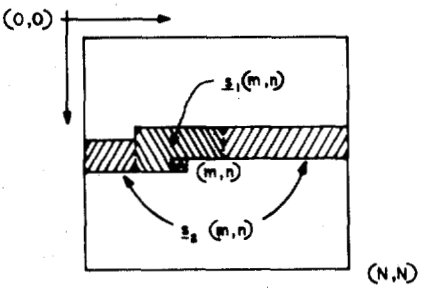

Fig. 1. Assignment of points to partioned state vector.

$$\begin{aligned}\boldsymbol{s}_1(m,n) \triangleq [&s(m,n), s(m-1,n), \cdots, s(m-M+1,n);\\ &s(m+M+1,n-1), \cdots, s(m-M+1,n-1); \cdots;\\ &s(m+M+1,n-M), \cdots, s(m-M+1,n-M)]^T.\end{aligned} \tag{6}$$

Also, we define $\boldsymbol{s}_2(m,n)$ to complete the partition of $\boldsymbol{s}(m,n)$:

$$\boldsymbol{s}(m,n) \triangleq \begin{bmatrix}\boldsymbol{s}_1(m,n)\\ \boldsymbol{s}_2(m,n)\end{bmatrix}. \tag{7}$$

The resulting assignment of the points is as shown in Fig. 1. Using the notation of [1] with $\boldsymbol{G} = \boldsymbol{I}$, the single row matrix $\boldsymbol{H}$, written as $\boldsymbol{h}^T$, and the single column matrix $\boldsymbol{K}$, written as $\boldsymbol{k}$, we have the following reduced update filter equations.

Prediction:

$m \to m+1$ (except at end of line where $m \to 1$ and $n \to n+1$)

$$\boldsymbol{P}_b(m,n) = \boldsymbol{C}\boldsymbol{P}_a(m-1,n)\,\boldsymbol{C}^T + \boldsymbol{Q}_w \tag{8}$$

$$\hat{\boldsymbol{s}}_{1b}(m,n) = \boldsymbol{C}_{11}\hat{\boldsymbol{s}}_{1a}(m-1,n) + \boldsymbol{C}_{12}\hat{\boldsymbol{s}}_{2a}(m-1,n). \tag{9}$$

Update:

$$\boldsymbol{k}_1(m,n) = \boldsymbol{P}_{11,b}\boldsymbol{h}_1(\boldsymbol{h}_1^T\boldsymbol{P}_{11,b}(m,n)\,\boldsymbol{h}_1^T + \sigma_v^2)^{-1} \tag{10}$$

$$\hat{\boldsymbol{s}}_{1a}(m,n) = \hat{\boldsymbol{s}}_{1b}(m,n) + \boldsymbol{k}_1(m,n)[r(m,n) - \boldsymbol{h}_1^T\hat{\boldsymbol{s}}_{1b}(m,n)] \tag{11}$$

$$\boldsymbol{P}_{1i,a}(m,n) = [\boldsymbol{I} - \boldsymbol{k}_1(m,n)\,\boldsymbol{h}_1^T]\,\boldsymbol{P}_{1i,b}(m,n), \qquad i = 1,2 \tag{12}$$

where the matrix and vector partitions $\boldsymbol{C}_{ij}$, $\boldsymbol{P}_{ij}$, and $\boldsymbol{k}_i$, $\boldsymbol{h}_i$ are similar to the partition of $\boldsymbol{s}$.

The scalar equations corresponding to models of (1) and (2) are obtained in [1] as specializations of the above vector equations for $\boldsymbol{h}_1^T = (1, 0, \cdots, 0)$ and $\boldsymbol{h}_2 = \boldsymbol{0}$. They are as follows.

Filtering:

$$\hat{s}_b^{(m,n)}(m,n) = \sum_{\mathcal{R}_{\oplus+}} c_{kl}\,\hat{s}_a^{(m-1,n)}(m-k, n-l) \tag{13}$$

$$\begin{aligned}\hat{s}_a^{(m,n)}(i,j) = \hat{s}_b^{(m,n)}(i,j) &+ k^{(m,n)}(m-i, n-j)\\ &\cdot [r(m,n) - \hat{s}_b^{(m,n)}(m,n)],\\ &(i,j) \in \mathcal{R}_{\oplus+}^{(m,n)}.\end{aligned} \tag{14}$$

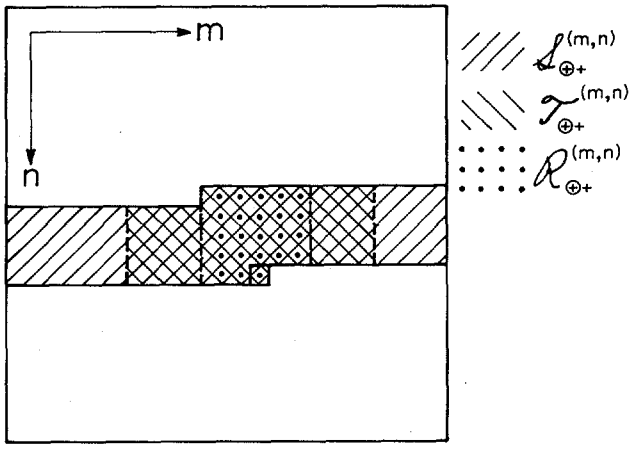

Fig. 2. Region assignment for $\mathcal{T}_{\oplus+}^{(m,n)}$, covariance update region.

Error Covariance and Gain:

$$R_b^{(m,n)}(m,n;k,l) = \sum_{\mathcal{R}_{\oplus+}} c_{op} R_a^{(m-1,n)}(m-o,n-p;k,l), \quad (k,l) \in \mathcal{S}_{\oplus+}^{(m,n)} \tag{15a}$$

$$R_b^{(m,n)}(m,n;m,n) = \sum_{\mathcal{R}_{\oplus+}} c_{kl} R_b^{(m,n)}(m,n;m-k,n-l) + \sigma_w^2 \tag{15b}$$

$$k^{(m,n)}(i,j) = R_b^{(m,n)}(m,n;m-i,n-j)/(R_b^{(m,n)}(m,n;m,n)+\sigma_v^2), \quad (i,j) \in \mathcal{R}_{\oplus+} \tag{16}$$

$$R_a^{(m,n)}(i,j;k,l) = R_b^{(m,n)}(i,j;k,l) - k^{(m,n)}(m-i,n-j) \cdot R_b^{(m,n)}(m,n;k,l), \quad (i,j) \in \mathcal{R}_{\oplus+}^{(m,n)}; \quad (k,l) \in \mathcal{S}_{\oplus+}^{(m,n)}. \tag{17}$$

These equations also use the notation of [1] where the superscript represents the step in the filtering and the argument represents the position of the data. Also in [1], the approximate reduced update equations are obtained by replacing the region $\mathcal{S}$ in (13)-(17) by a much smaller region $\mathcal{T}$ of fixed size independent of the image size N. This is shown in Fig. 2. This approximation assumes negligible source correlation at large distances and, thus requires a stable dynamical model. The approximation works quite well in practice for the many models tested. Typically $\mathcal{T}$ can be chosen as small as a few columns wider than the updated region.

III. Extension to Image Restoration

In image restoration the observation (2) is modified to reflect a transformation on the signal, which specialized to the linear shift-invariant (LSI) case becomes

$$r(m,n) = \sum_{kl} h_{kl} s(m-k,n-l) + v(m,n). \tag{18}$$

For a particular support of the distorting system h, (18) can be put into the form (4). Namely, the support of h must be restricted to $\mathcal{R}_{\oplus+}$. If additionally the support of h is small enough, it can be represented as $\boldsymbol{h}$ with $\boldsymbol{h}_2 = \mathbf{0}$, and hence, is in the class of problems to which the reduced update vector equations (8)-(12) apply. If we slightly enlarge the local state (6) on the left with one more column from the global state (5), i.e., $[s(m-M,n), s(m-M,n-1), \cdots, s(m-M,n-M)]^T$, h can be an $(M \times M)$th order $\oplus+$ FIR filter. In the sequel we will assume that this has been done.

One can obtain the observational model h in various ways, e.g., least squares estimation [5], maximum-likelihood methods [6], and 2-D filter design [7]. The FIR constraint on h is particularly appropriate for motion blurs and finite size aperture effects. Zero-phase transformations may be incorporated in the model by tacitly agreeing to accept a small known shift in the output estimate.

A vector recursive method for image restoration was developed in [10] which has a scanner implementation similar to that proposed here. However, with reference to [10, Eq. (4)], it can be seen that their constrained (reduced) update formulation is not based on a general recursive signal model since it does not include previously computed points on the same line. Furthermore, when a general NSHP model is used in the scanner processor of [10], the order of the resulting Kalman prediction is not determined. However, their example involving a (1×1)th order ++ model indicates that it may be quite large.

Assuming h is an NSHP FIR filter of order $(M \times M)$ or less, we have (18) equivalent to (2) with $\boldsymbol{h}_2 = \mathbf{0}$ and

$$\boldsymbol{h}_1^T = [h_{0,0}, \cdots, h_{-M,0}; h_{M,-1}, \cdots, h_{-M,-1}; \cdots; h_{M,-M}, \cdots, h_{-M,-M}]. \tag{19}$$

Then the 2-D RUKF applies to this problem. Converting over to the computationally more efficient scalar equations, we obtain the following.

Filtering:

$m \to m+1$ (except at end of line)

$$\hat{s}_b^{(m,n)}(m,n) = \sum_{\mathcal{R}_{\oplus+}} c_{kl} \hat{s}_a^{(m-1,n)}(m-k,n-l); \quad (m,n) \in [1,N]^2 \tag{20}$$

$$\hat{s}_a^{(m,n)}(i,j) = \hat{s}_b^{(m,n)}(i,j) + k^{(m,n)}(m-i,n-j) \cdot \left[r(m,n) - \sum_{\mathcal{R}_{\oplus+}} h_{kl} \hat{s}_b^{(m,n)}(m-k,n-l) \right]; \quad (i,j) \in \mathcal{R}_{\oplus+}^{(m,n)}. \tag{21}$$

Error Covariance and Gain: Prediction same as (15)

$$k^{(m,n)}(i,j) = \frac{\sum_{kl} h_{kl} R_b^{(m,n)}(m-k,n-l;m-i,n-j)}{\sum_{kl}\sum_{ij} h_{kl} h_{ij} R_b^{(m,n)}(m-k,n-l;m-i,n-j) + \sigma_v^2}; \quad (i,j) \in \mathcal{R}_{\oplus+} \tag{22}$$

$$R_a^{(m,n)}(i,j;k,l) = R_b^{(m,n)}(i,j;k,l) - k^{(m,n)}(m-i,n-j) \cdot \sum_{op} h_{m-o,n-p} R_b^{(m,n)}(m-o,n-p;k,l);$$

$$(i,j) \in \mathcal{R}_{\oplus+}^{(m,n)}, \quad (k,l) \in \mathcal{S}_{\oplus+}^{(m,n)}. \quad (23)$$

Equations (20)-(23) and (15) constitute the RUKF for deconvolution problems. The equations are seen to be very similar to (13)-(17) for estimation problems when signal distortion is not present. In fact, the equations associated with prediction are unchanged and those associated with updating are modified only by convolution with the kernal h in appropriate places. This is analogous to the one-dimensional case. Experimental results are presented in Section V.

As in Section II, this deconvolution version of the RUKF equations applies for the case of zero boundary conditions on the zero-mean field $s(m,n)$. In many applications, including image restoration, it is more natural to consider random boundary conditions. In the next section, the RUKF is extended to the case of random boundary conditions.

IV. Boundary Conditions

The initial condition problem for 1-D Kalman filtering is to select an optimal initial estimate of the state, along with its associated initial error covariance. Often this estimate is simply the mean of the signal process as would be appropriate, for example, when no *a priori* information is available. When the data set is finite, a boundary value problem consisting of both initial and final conditions must, in general, be considered [see Fig. 3(a)]. If one has a finite length section of an infinite length data set, the causal filtering problem ignores any final conditions, thus enabling one to reduce the general boundary condition problem to an initial value problem. Hence, the two-point boundary nature of a finite length data set can be ignored in the 1-D case by the expedient of causal filtering. The general 2-D boundary condition set is shown in Fig. 3(b) where we denote the image or observation set by I and boundary set by B. Unlike its 1-D counterpart, this boundary condition problem does not degenerate to an initial condition problem for causal filtering. This is because the data scan causes the boundaries to be encountered repetatively in the course of the filtering, at the beginning and end of each scan line. Thus, in addition to initial conditions at the top and final conditions on the bottom, the majority of the boundary consists of points that cannot be so categorized and therefore really has no 1-D counterpart. Therefore, unlike the 1-D case, a causal 2-D filter cannot ignore the boundary condition nature of the problem.

Fig. 4 shows the minimum boundary condition set to uniquely specify the output of an NSHP recursive estimator or filter on a square region.[1] The boundary condition set is much more than an initial condition set.

[1]We note parenthetically that a quarter-plane recursive estimator or filter would require the boundary conditions of Fig. 4, with the exception of those on the right-hand side. This somewhat simpler situation is qualitatively unchanged from the general NSHP case to be presented here.

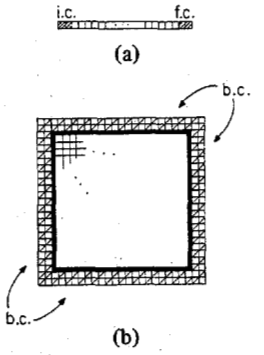

Fig. 3. Finite data sets and their general boundary condition sets.

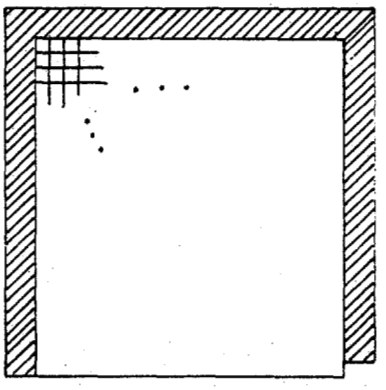

Fig. 4. Minimum boundary condition region (shaded) for NSHP estimator or filter on square region.

In performing 2-D recursive estimation, for random boundary conditions, one has the following options.

1) Estimate the boundary values based on past and present data.

2) Ignore the randomness of the boundary values and fix them at their mean value.

In this regard, various questions arise. How does one do 2-D Kalman filtering in the presence of these random boundary conditions? What is the practical importance of the boundary conditions for reasonable image models? Should the global state vector be modified for the case of random boundary conditions? We will answer these questions below.

We assume in this section that the boundary conditions are sets of random variables, since, if the boundary conditions are deterministic, only straightforward modifications to methods already presented are needed. In particular, the method presented in [1] and Sections II and III, where the boundary conditions are taken to be zero, can be modified by simply inserting the known boundary values into the equations when needed. This is completely analogous to the 1-D Kalman filter with deterministic input, and, in fact, through the raster scanning is equivalent to it. In this way one can accomplish option 2).

The case of random boundary conditions is very realistic, especially for images of objects extending beyond the field of view. Random boundary conditions are also necessary to properly characterize a square region obtained from a homogeneous random field. Taking option 1), one can modify the 2-D Kalman filter to estimate the boundary values. One way

to do this was presented in [10]. It consisted of separate realizations of the left and right boundary fields as vector Markov processes. However, this approach is only approximate and can seldom be made exact. Furthermore, the approximation is not appropriate for many applications. We now elaborate on these ideas and then develop an alternative treatment of the boundary fields which does not suffer from these problems.

A. Predicting Boundary Values

The following notations and definitions will prove helpful.

Notation: Let $I_N^-(m,n)$ and $B_N^-(m,n)$ denote the past of the image and boundary respectively at pixel (m,n) as shown in Fig. 5. We abbreviate this as I^- and B^- whenever no confusion can arise. Let $s_b^L(n)$ and $s_b^R(n)$ denote vectors of left-hand and right-hand boundary values, respectively, at line n with a depth of M lines.

Definition: A random boundary field will be called *conditionally independent* if

$$E[s_b^{(\cdot)}(n)|s \text{ on } I^- \cup B^-] = E[s_b^{(\cdot)}(n)|s_b(n-1)]$$

for all n. Otherwise, it will be called *conditionally dependent.*

By way of example, it is easy to see that the boundary fields of [10] are conditionally independent by the partitioned nature of their equation (6). To find a boundary field that is conditionally dependent, consider the field to be jointly homogeneous on $I \cup B$ with NSHP model coefficients $c_{01} = c_{11} = c_{10} = \epsilon$ and $c_{-1,1} = 0.9$ with $|\epsilon| < 0.03$. Clearly, since $|\epsilon|$ is very small, the most important term in the prediction of $[s_b^L(n)]_0 \equiv s(0,n)$ is $s(1,n-1)$ which is not in B. While this is an extreme example, it can be expected that many cases of interest will not be adequately modeled with conditionally independent boundary fields. In particular, one can show the following general result.

Theorem 1: If $I \cup B$ is a segment from a homogeneous Gaussian random field, then the boundary field will be conditionally independent iff the model is a 1-D vertical, scalar model (i.e., $\oplus$+). Otherwise, the prediction $E[s_b^{(\cdot)}(n)|s$ on $I^- \cup B^-]$ will be of $O(nM)$ order.

Proof: Letting "$\sim$" denote equivalence for prediction purposes, we have

$$\{s\}_{I^- \cup B^-} \sim \{s\}_{B^-} \cup \{w\}_{I^-}.$$

Then

$$\begin{aligned} E[s(0,n)|\{s\}_{I^- \cup B^-}] &= E[s(0,n)|\{s\}_{B^-} \cup \{w\}_{I^-}] \\ &= E[s(0,n)|\{s\}_{B^-}] + E[s(0,n)|\{w\}_{I^-}] \end{aligned} \tag{24}$$

by the orthogonal projection theorem since $\{s\}_{B^-} \perp\!\!\!\perp \{w\}_{I^-}$, i.e., they are jointly independent.

Now to prove our theorem, we will show that, in general, $E[s(0,n)|\{w\}_{I^-}]$ is not zero and in fact is a $O(nM)$ order combination of the past values of s on the left-hand strip shown shaded in Fig. 6.

Since $\{w\}_{I^-}$ is jointly orthogonal, we may write

$$E[s(0,n)|\{w\}_{I^-}] = \sum_{(k,l) \in I^-} (\delta - c)^{-1}(-k, n-l)\, w(k,l)$$

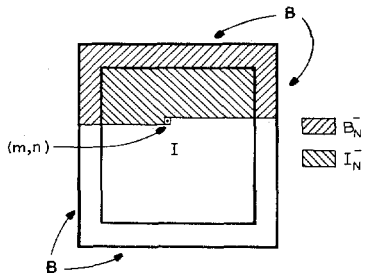

Fig. 5. Diagram illustrating the regions $I_N^-(m,n)$ and $B_N^-(m,n)$.

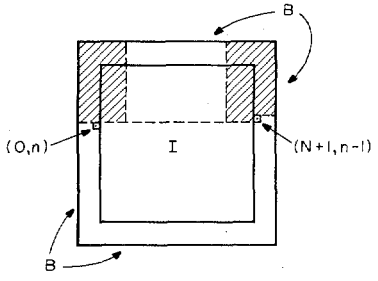

Fig. 6. Diagram illustrating support of boundary predictions (shaded areas) for causal (i.e., raster) scans.

where δ is the 2-D delta sequence and $(\cdot)^{-1}$ denotes an operator inverse.

Rewriting in terms of s, we obtain

$$\begin{aligned} E[s(0,n)|\{w\}_{I^-}] = \sum_{(k,l) \in I^-} &((\delta - c) * s)(k,l) \\ &\cdot (\delta - c)^{-1}(-k, n-l). \end{aligned}$$

Rewriting this equation further as a weighting of s on $I^- \cup B^-$

$$E[s(0,n)|\{w\}_{I^-}] = \sum_{(o,p) \in I^- \cup B^-} \alpha_{op}\, s(o,p)$$

where

$$\alpha_{op} \triangleq \sum_{(k,l) \in I^-} (\delta - c)(k-o, l-p) \cdot (\delta - c)^{-1}(-k, n-l).$$

Since the dynamical model is $(M \times M)$th order $\oplus$+, the restriction $(k,l) \in I^-$ has no effect for $o \geq M$, and hence for such o, $\alpha_{op} = \delta(-o, n-p) = 0$. For $1 \leq o < M$, the restriction removes part of the left-hand side of $(\delta - c)$ from the sum. Hence, $(\delta - c)^{-1}$ is no longer its causal, translated inverse. This implies that $\alpha_{op} \neq 0$ in general for $1 \leq o < M$ and for all $1 \leq p < n$. The only exception is if the model is ++ or quarter plane causal, for the $(\delta - c)$ has no left-hand side. Repeating the argument on the right-hand boundary, we conclude that the model must be $-$+ as well as ++, hence, $\oplus$+, in the notation of [4].

It is evident from this theorem that conditionally independent boundary fields are not appropriate for recursively estimating segments I of homogeneous random fields. Furthermore, we note that, in general, the boundary prediction requires a growing support not contained in the global state of (5). Returning to the 2-D Kalman filtering problem, this theorem tells us that in general we must augment the global state vector s by the

shaded region in Fig. 6, to provide the missing equations

$$s_b^R(n-1) = C^R s^*(N, n-1) + w^R(n-1) \quad (25)$$

$$s_b^L(n) = C^L s^*(N, n-1) + w^L(n) \quad (26)$$

needed to predict the boundary values required by (3) near the boundary. Here s^* is the global state vector augmented to include the shaded regions shown in Fig. 6, C^R and C^L are the relevant prediction matrices and $w^R(n-1)$ and $w^L(n)$ are the prediction errors. Since the sequence

$$\{w(1,1), \cdots, w(n,1), w^R(1), w^L(2), w(1,2), \cdots, w(N,2), w^R(2), \cdots\}$$

constitutes a causal prediction error sequence based on all the past data, it follows that this vector sequence is white and that (3) with s^* in place of s together with (25) and (26) constitute an appropriate innovations sequence for the scalar scanned data. Applying Kalman filtering to this sequence, we see that the boundary prediction will be $O(nM)$ order unless the data model is $\oplus+$. Thus, we have the following corollary to Theorem 1.

Corollary: Let $\hat{s}^*(m,n)$ be the causal, conditional mean estimate of the global state as augmented in (25) and (26), based on observations on I^-. Then the boundary estimate processes $\{\hat{s}_b^R(n-1), \hat{s}_b^L(n)\}$ will be conditionally independent iff the dynamical model of the signal (1) is $\oplus+$. Otherwise, the prediction step in the boundary estimation will be of $O(nM)$ order.

Since the dynamical model for s will almost never be $\oplus+$, the boundary estimates will almost never be conditionally independent, and the boundary prediction step in the 2-D Kalman filter will be $O(nM)$ order at the beginning and end of each scan line of observed data. This destroys the low order $O(M^2)$ prediction property that 2-D Kalman filters have inside the image I. Of course, one can approximate these boundary prediction steps by truncating the predictor support to that of the global state.

B. Augmenting Global State

An alternative to the above approach is to define the global state as shown in Fig. 7. This state includes all the boundary values needed to compute the future response and, thus avoids the need for the $O(nM)$ prediction at the start and end of each scan line. This global state is consistent with the 2-D state variable models of Roesser [11] and Kung *et al.* [12]. Since the prediction steps are always $O(M^2)$ order, the entire calculation can be made efficient by employing reduced update procedures for updating the global state. In this case the computation per point of the steady-state filter is not increased. Using the Corollary to Theorem 1 we can establish the following result.

Theorem 2: Let a scalar 2-D Kalman filter be used to recursively estimate on $I \cup B$ a homogeneous random field observed on I. Let the boundary field be conditionally dependent. Then initial and final prediction steps for each scan line will be of growing order $O(nM)$ unless the global state is augmented to include the boundary values necessary to determine future responses (see Fig. 7).

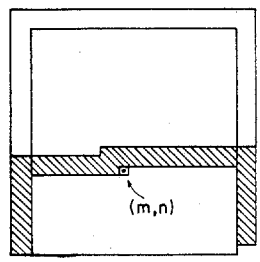

Fig. 7. Augmented state vector for random boundary conditions.

Proof: For each scan line, the initial prediction step must predict $s_b(n)$ iff its not in the global state. By the corollary to Theorem 1, this prediction will be of order $O(nM)$. The same argument applies to the boundary estimates at the end of the scan line. Since this holds for each n, the result follows.

To pursue this alternative, we modify the global state to include those boundary values which will be needed in the future. To completely characterize the future response, the state vector at (m,n) must have support as shown in Fig. 7. This global state vector is that of [1] and Sections II and III augmented by the set of boundary values to be needed in the future. This augmented global state will permit updating those boundary values to be involved in future estimates. The 2-D Kalman filter for this augmented global state is derived, as before, through a raster scanning argument converting the 2-D problem into an equivalent 1-D problem. For all those points in I, we have

$$s'(m,n) = C' s'(m-1,n) + w'(m,n) \quad (27)$$

where the augmented global state vector s' is given as

$$s'(m,n) \triangleq \begin{bmatrix} s(m,n) \\ b(m,n) \end{bmatrix} \quad (28)$$

with prior statistics

$$E[w'(m,n)] = \mathbf{0} \quad (29)$$

$$\text{cov}\{w'(m,n), w'(k,1)\} = Q_w \delta_k(m-k, n-1) \quad (30)$$

$$E[s'(o,o)] = E[b] = \mathbf{0} \quad (31)$$

$$\text{var}\{b\} = R_{ss} \quad (32)$$

where the covariance matrix R_{ss} is determined by the correlation function of the homogeneous random field s. Thus, we treat the case where s is homogeneous on $I \cup B$.

No boundary values are actually calculated by (27), the partition of the C' matrix being such that the $b(m,n)$ undergo an identity transformation. Their presence only permits the calculation of $s(m,n)$ near the beginning and end of lines, where the model support overlaps the boundary condition set. The augmented global state thus does not change the prediction step of the 2-D Kalman filter except that the presence of the boundary values in the global state will allow the calculation of error cross covariances between the data and boundary values. The Kalman filter, in turn, will then be able to calculate optimal updates of both the boundary values and the data values.

Note that the global state vector reduces in size as it pro-

gresses down the picture. However, this presents no particular problem with the mathematics, since the Kalman filter is recursively derived from point to point. If we define the σ-field of past and present observations $\mathcal{F}^{N}_{m,n} \triangleq \{r(k,l)$ on $I_N^- \cup (m,n)\}$, we find the following corrolary to Theorem 2.

Corollary: The 2-D Kalman filter estimate, using the augmented global state, is the causal conditional mean estimate

$$\hat{s}_a(m,n) = E[s(m,n)|\mathcal{F}^{N}_{m,n}].$$

The best causal estimate based on I_N can be shown to be asymptotic as $N \to \infty$ to the best estimate based on $\mathcal{R}_{++}$. Thus, if we let $\hat{s}(m,n) \triangleq E[s(m,n)|\mathcal{F}^{\infty}_{m,n}]$ we can show the following result.

Theorem 3: Let $E\|s(m,n)\|_1 < \infty$. Then the 2-D Kalman filter, based on the augmented global state, is asymptotically optimum as $I_N \to I_\infty = \mathcal{R}_{++}$, i.e.,

$$\hat{s}_a(m,n) \to E[s(m,n)|\mathcal{F}^{\infty}_{m,n}] \quad \text{with probability 1.}$$

Proof: From the corollary to Theorem 2,

$$\hat{s}_a(m,n) = E[s(m,n)|\mathcal{F}^{N}_{m,n}].$$

So since

$$\mathcal{F}^{N}_{m,n} \subset \mathcal{F}^{N+1}_{m,n} \subset \cdots \subset \mathcal{F}^{\infty}_{m,n},$$

we have by a standard convergence Theorem [8]

$$E[s(m,n)|\mathcal{F}^{N}_{m,n}] \to E[s(m,n)|\mathcal{F}^{\infty}_{m,n}].$$

C. RUKF with Boundary Update

The 2-D Kalman filter, while optimal in the causal sense for the assumed total ordering, is computationally intractable for reasonably large sized images. The 2-D RUKF limits updates to the nearby points, supposed to be of high correlation, and omits wasteful updating of distant points supposed to be only slightly correlated with the present observation. On deciding to update only a part of the augmented global state at any point, the derivation goes through analogously to that of [1]. Thus, we obtain equations of the same form as (8)-(12) where s_1 is the updated part of the augmented global state vector and s_2 is the nonupdated part.

The scalar equations for this RUKF on the augmented global state are the same as (15) and (20)-(23) with the exception that the range of indexes changes slightly to accommodate the enlarged global state. By letting the 2-D lattice extend out into the boundaries, we can represent both the boundary values and nonboundary values by the same symbols. Taking the filtering equations first, (20) would remain unchanged with the understanding that boundary estimates be inserted into the right-hand side when $\mathcal{R}^{(m,n)}_{\oplus+}$ overlaps the boundary. Equation (21) would consist of updates of both data estimates and boundary estimates. The gain equation (22) and error covariance equations (15) and (22)-(23) would be changed accordingly. Notationally, all that needs to be done is to define $\mathcal{U}^{(m,n)}_{\oplus+}$ the update region on both the data and the boundary and $\mathcal{S}^{(m,n)}_{\oplus+}$ as the augmented global state region. Then the equations (15) and (20)-(23) hold exactly as written with $\mathcal{U}^{(m,n)}_{\oplus+}$ substituted for $\mathcal{R}^{(m,n)}_{\oplus+}$. Such an update region is depicted in Fig. 8 for three points on a scan line, corresponding

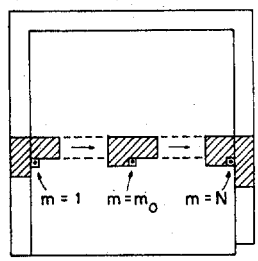

Fig. 8. The update region at (m,n), $\mathcal{U}^{(m,n)}_{\oplus+}$ for several values of m.

TABLE I
SIGNAL-TO-NOISE RATIOS AND IMPROVEMENTS

Image Blur Model	Input SNR (dB)	Output SNR (dB)	Improvement (dB)
(3 × 3) Model	11.8	21.3	9.5
(4 × 4) Model	9.4	15.9	6.5
(7 × 1) Model	10.9	15.0	4.1

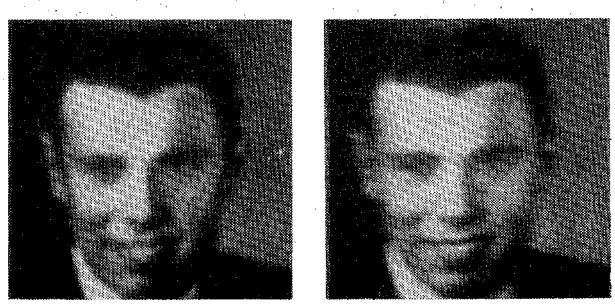

(a) (b)

Fig. 9. Noisy blurred images: (a) (4 × 4) blur; (b) (7 × 1) blur.

to the first point $m = 1$, a generic point m_o, and the last point $m = N$. As before, the filter gain computation then becomes very efficient, however, the error covariance computation per point is still of order $O(N)$. At this stage an approximate fixed size region $\mathcal{T}^{(m,n)}_{\oplus+}$ is substituted for $\mathcal{S}^{(m,n)}_{\oplus+}$ in the error covariance computations. The resulting approximate RUKF will have fixed error covariance computation per point independent of image size. In the next section experimental results are presented on the use of the approximate 2-D RUKF.

V. EXPERIMENTAL RESULTS

This section presents experimental results on both image restoration and on boundary condition effects.

A. Image Restoration

The original signal was a (128 × 128) head-and-shoulders image data field, quantized to 8 bits (256 gray levels). Blurred images were generated using uniform spread functions of finite extent. These point-spread functions correspond to a finite size uniform aperture (3 × 3 and 4 × 4 models) or to linear motion blur (7 × 1 model). Measurement noise $w(n)$ was then added to the blurred images using a Gaussian white noise generator. For simulation purposes, the blurred signal-to-noise ratio was set to 40 dB. The total input signal-to-noise ratios, including the blurring, are listed in Table I. The noisy blurred images are shown in Fig. 9.

(a) (b)

Fig. 10. Enhanced images: (a) (4 × 4) blur; (b) (7 × 1) blur.

These images were processed using the algorithm of Section III. For estimation, a stationary ⊕+ NSHP filter of appropriate order (i.e., a second-order filter for 3 × 3 model and a third-order filter for 4 × 4 and 7 × 1 models) was considered, the parameters of which were derived from the least squares identification approach [9]. In order to improve the program efficiency and to reduce the memory storage, the error covariance processing and gain calculation part of the filter was decoupled from the picture processing part. The error covariance processing program was first used to design the filter by iterating towards convergence. The steady state was achieved within a percent or two after 10 rows and 20 columns for the second-order filter, and after 15 rows and 25 columns for the third-order filter. In this design, the reduced update of the error covariance matrix was limited to the $\mathcal{T}_{\oplus+}$ region of half-width equal to 5 for the second-order filter and to 7 for the third-order filter. The noisy blurred images were then processed using the resulting steady-state RUKF's. The processed images are shown in Fig. 10. The results, in the form of measured SNR improvement, are shown in Table I.

As seen from Table I, there is a considerable amount of improvement in the mean-square error. This improvement is highest for the (3 × 3) point-spread function model (not shown). The subjective improvement is very good, making the restored image visually nearly the same as the original. In the case of the (7 × 1) and (4 × 4) point-spread functions, both the numerical and subjective results are less than perfect. Ringing arises due to the signal and noise exciting peaks in the response of the deconvolution filter. Subjectively, the results are still quite dramatic in the increased sharpness of the restored images. Some further subjective improvement could probably be obtained by optimizing over the design signal-to-noise ratio parameter.

One caution in interpreting these results is that, since this is a simulation, the point-spread function is known exactly. If it were not known exactly, performance would be degraded.

B. Boundary Conditions

To test the theory of boundary condition effects, given in Section IV, simulations were carried out on homogeneous random fields generated by an autoregressive image model. This model was derived from the face image. Measurement noise $w(n)$ was added to this random field using a Gaussian white noise generator at signal-to-noise ratio equal to 3 dB.

Since no *a priori* knowledge of the boundary conditions was assumed, they were initially set to the mean of the field, zero. Thus, the initial conditions for the error covariance matrix were set to the image covariance derived from the image model. A raised-cosine window was applied to these boundary covariance values to lessen the region truncation effects near and on the boundary. The parameters of the 2-D raised-cosine window were adjusted to give optimum performance. This window is needed because initially the error covariance at the boundary is not highly peaked, otherwise one would need a much larger $\mathcal{T}$ region near the boundary.

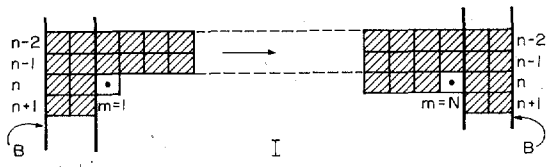

Fig. 11. Regions used in boundary update simulation.

A second-order ⊕+ NSHP model support $\mathcal{R}$ was used. The support of the update region $\mathcal{U}$, inside the image, was taken to be one column wider on each side. Near a boundary, however, this support bends according to Fig. 11, for the first and the last point on a scan line. Thus, the support spans the next line near the boundary for near optimal prediction estimates. The error covariance update regions, $\mathcal{T}_{\oplus+}$, were chosen accordingly.

The random fields were then processed using the reduced update filter with the above boundary conditions and update region supports. An error covariance processing program was first used to design the filter by iterating towards a steady state. The steady-state gain vectors were stored for the first 10 columns from the right- and left-hand boundaries and were subsequently used for filtering along with a steady-state gain vector for the field away from the boundary. The mean-square errors for filtered and smoothed estimates were then measured.

The result of filtering with a RUKF designed assuming fixed boundary conditions, referred to as option 2) in Section IV, was also computed. Here the boundary was assumed to be deterministic and hence was held at the mean, zero. Accordingly, the initial conditions for the error covariance were also set to zero and were not subsequently updated. As a result, the theoretical error covariance will increase with distance from the boundary. Conversely, the experimentally observed error covariance will decrease with distance from the boundary since the boundary is really random.

Two more filters were run on the same data for further comparison. First, the steady-state RUKF was run to determine its suboptimality near the boundary. Second, an optimum FIR nonrecursive filter was used to estimate the data values near the boundary. An 8 × 8 filter, in the sense of using the last 8 lines and the first 8 columns, was found adequate for this purpose.

The filtering results on 30 separate realizations were then averaged to produce the results shown in Fig. 12. Here the improvements (dB) for each filter were plotted versus the image column index for the first five columns on the left. (Similar results hold near the boundary on the right.) Fig. 12(c) and (d) shows results for the filtered-with-delay or smoothed estimate. (A smoothed FIR estimate was not calculated.) Fig.

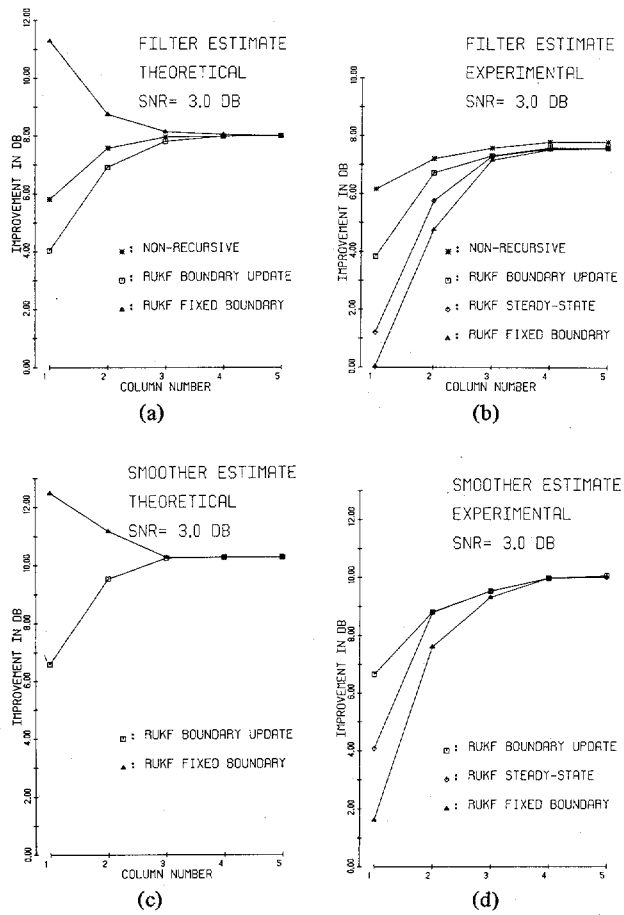

Fig. 12. Filter improvement versus column index; (a) filter estimate (theoretical); (b) filter estimate (experimental); (c) smoother estimate (theoretical); (d) smoother estimate (experimental).

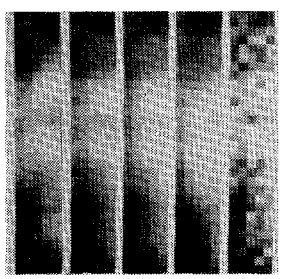

Fig. 13. Close up of filtered random field showing effect of treatment of boundary conditions. Strip order: original, boundary update RUKF, steady-state RUKF, fixed boundary RUKF, noisy image.

12(a) and (c) shows theoretical improvements predicted by the design algorithm (i.e., the error covariance equations) while Fig. 12(b) and (d) show the experimentally observed improvement. It is clear that significant improvement can be obtained near the boundaries by taking account of the randomness of the boundary conditions. We see that the steady state RUKF performs fairly well. Finally, we see that the optimal FIR filtered estimate is best in column 1 by 2 dB over the RUKF with boundary update. It is felt that this additional error can only be reduced by the expense of a much larger update $\mathcal{U}$ and $\mathcal{T}$ region when very near a boundary.

Fig. 13 shows these results visually using a close-up of the image near the boundary. The order of the strips is (left-to-right): original image, RUKF with boundary update, steady-state RUKF, fixed boundary RUKF, noisy image. The improvement due to boundary update is clearly evident in the first or second column.

VI. Conclusions

The 2-D RUKF was extended to image restoration/deconvolution type problems. A more comprehensive treatment of 2-D boundary conditions was introduced. Then simulation examples were presented to confirm the theory.

References

[1] J. W. Woods and C. H. Radewan, "Kalman filtering in two-dimensions," *IEEE Trans. Inform. Theory*, vol. IT-23, pp. 473–482, July 1977.

[2] J. W. Woods, "Correction to 'Kalman filtering in two-dimensions,'" *IEEE Trans. Inform. Theory*, vol. IT-25, pp. 628–629, Sept. 1979.

[3] H. C. Andrews and B. R. Hunt, *Digital Image Restoration.* Englewood Cliffs, NJ: Prentice-Hall, 1977.

[4] M. P. Ekstrom and J. W. Woods, "Two-dimensional spectral factorization with applications in recursive digital filtering," *IEEE Trans. Acoust., Speech, Signal Processing*, vol. ASSP-24, pp. 115–128, Apr. 1976.

[5] R. A. Wiggins, "On factoring the correlations of discrete multivariable stochastic processes," Ph.D. dissertation, Dep. Geology Geophys., M.I.T., Cambridge, MA, 1965.

[6] W. E. Larimore, "Statistical inference on stationary random fields," *Proc. IEEE*, vol. 65, pp. 961–970, June 1977.

[7] D. B. Harris and R. M. Mersereau, "A comparison of algorithms for minimax design of two-dimensional linear phase FIR digital filters," *IEEE Trans. Acoust. Speech, Signal Processing*, vol. ASSP-25, pp. 492–500, Dec. 1977.

[8] R. S. Liptser and A. N. Shiryayev, *Statistics of Random Processes I General Theory.* New York: Springer-Verlag, 1977, p. 17.

[9] V. K. Ingle, A. Radpour, J. W. Woods, and H. Kaufman, "Recursive estimation with nonhomogeneous image models," in *Proc. 1978 IEEE Conf. Pattern Recognition and Image Processing*, Chicago, IL, May 1978, pp. 105–108.

[10] M. S. Murphy and L. M. Silverman, "Image model representation and line-by-line recursive restoration," *IEEE Trans. Automat. Contr.*, vol. AC-23, pp. 809–816, Oct. 1978.

[11] R. P. Roesser, "A discrete state-space model for linear image processing," *IEEE Trans. Automat. Contr.*, vol. AC-20, pp. 1–10, Feb. 1975.

[12] S. Y. Kung, B. C. Levy, M. Morf, T. Kailath, "New results in 2-D systems theory, part II," *Proc. IEEE*, vol. 65, pp. 945–961, June 1977.

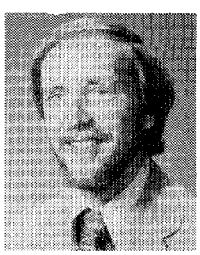

John W. Woods (S'67–M'70) was born in Washington, DC, on December 5, 1943. He received the B.S., M.S., E.E., and Ph.D. degrees in electrical engineering from the Massachusetts Institute of Technology, Cambridge, MA, in 1965, 1967, 1967, and 1970, respectively.

From 1970 to 1973 he was at the VELA Seismological Center, Alexandria, VA, working on array processing of digital seismic data. From 1973 to 1976 he was at the Lawrence Livermore Laboratory, University of California, working

on two-dimensional digital signal processing. Since 1976 he has been with the Department of Electrical and Systems Engineering, Rensselaer Polytechnic Institute, Troy, NY, where he is currently an Associate Professor. He has taught courses in digital signal processing, stochastic processes, information theory, and communication systems. His research interests include estimation, detection, recursive filtering and source encoding of multidimensional data.

Dr. Woods was co-recipient of the 1976 Senior Award of the IEEE Acoustics, Speech, and Signal Processing Society. He is a member of the Acoustics, Speech, and Signal Processing Technical Committee on Digital Signal Processing. He is an Associate Editor for Signal Processing for the IEEE TRANSACTIONS ON ACOUSTICS, SPEECH, AND SIGNAL PROCESSING. He is also a member of Sigma Xi, Tau Beta Pi, Eta Kappa Nu, and the AAAS.

Vinay K. Ingle (S'77-M'80) was born in Bombay, India, on December 20, 1953. He received the B.Tech. degree with distinction in electrical engineering from Indian Institute of Technology, Bombay, in 1976, and the M.S. degree in electrical engineering from Illinois Institute of Technology, Chicago, in 1977. He is currently working towards the Ph.D. degree at Rensselaer Polytechnic Institute, Troy, NY.

Since 1977 he has been a Research Assistant in the Department of Electrical and Systems Engineering, Rensselaer Polytechnic Institute. His research interests include detection, estimation, two-dimensional signal processing, and real-time processing of images.

Zero Sets of Multiparameter Functions and Stability of Multidimensional Systems

EZRA ZEHEB, SENIOR, MEMBER, IEEE, AND EUGENE WALACH

Abstract—**New theorems, which can be used to find the zero set of a multiparameter rational function of a complex variable where the distinguished boundary of the parameters' closed domain of definition is composed of piecewise smooth Jordan arcs or curves, are stated and proved.**

The results are used to derive a new simplified procedure for a multidimensional stability test, presented for the continuous-analog case, as well as for the discrete-digital case. Now proofs to Huang's and Strintzis' theorems on multidimensional stability are also provided, as an application of the theorems on zero sets.

I. INTRODUCTION

INTEREST in multivariable systems and multidimensional filters has recently arisen, as expressed and summarized in a special issue of the PROCEEDINGS OF THE IEEE [1] on the subject, and numerous articles thereafter, to name but a few [2]-[6], [21].

The root locus method [7], [8], which is well developed and is easily implemented both manually and computerwise [9] has been very successfully applied to a wide variety of problems, necessitating some knowledge of the roots of a rational function of a complex variable, which depends on a real parameter. Unfortunately, with a few exceptions [10], there have not been many expansions of this powerful method to the case where there are more than one parameter, and not necessarily real. Such a tool could prove very useful in simplifying test procedures and deriving new results in topics, such as design and stability of multidimensional digital and continuous filters, and, presumably, design of variable or distributed-lumped networks, through the multivariable positive real concept [11], [12]. In fact, some related ideas to the multiparameter root loci concept have already led to some advantageous procedures to test positivity and nonnegativity of multivariable real polynomials [13], a problem which stems partly from the above mentioned topics.

In Section II of the present paper, the authors present new theorems which enable one to find the zero set of a multiparameter rational function of a complex variable, where the boundary of each parameter's domain of definition, in the closed complex plane, is closed and composed of piecewise smooth Jordan arcs or curves.

Another proof of Huang's [14] theorem for stability of two-dimensional filters is a simple outcome of these theorems.

In Section III, the previous line of thought is used to provide a new proof to Strintzis' [5] theorem.

In Section IV, the theorems of Section II are used to derive a new simplified necessary and sufficient condition for the test

$$Q(jx) = Q(jx_1, \cdots, jx_n) \neq 0 \qquad \forall x \in R^n$$

Manuscript received November 12, 1979; revised August 19, 1980. The last stages of this work were carried out by E. Zeheb while visiting the University of Natal, Durban, RSA, under an NCRD/CSIR contract.

The authors are with the Department of Electrical Engineering Technion, Israel Institute of Technology, Haifa, Israel.

0096-3518/81/0400-0197$00.75